

**UCSF**

**UC San Francisco Electronic Theses and Dissertations**

**Title**

Drug capture efficacy using polystyrenesulfonate-coated chemofilter device

**Permalink**

<https://escholarship.org/uc/item/7mw3s8nm>

**Author**

Decavel-Bueff, Emilie

**Publication Date**

2019

Peer reviewed|Thesis/dissertation

Drug capture efficacy using polystyrenesulfonate-coated chemofilter device

by  
Emilie Decavel-Bueff

THESIS  
Submitted in partial satisfaction of the requirements for degree of  
MASTER OF SCIENCE

in  
Biomedical Imaging

in the  
GRADUATE DIVISION  
of the  
UNIVERSITY OF CALIFORNIA, SAN FRANCISCO

Approved:

DocuSigned by:  
*Steven Hetts* Steven Hetts  
DA41E0D34A4A463... Chair

DocuSigned by:  
*Mark Wilson* Mark Wilson

DocuSigned by:  
*Susan Noworolski* Susan Noworolski

DocuSigned by:  
*Alastair Martin* Alastair Martin  
0D642C3C2048404...

---

Committee Members

Copyright 2019  
By  
Emilie Decavel-Bueff

## **Acknowledgements**

I would like to thank my Thesis Committee, Drs. Steven Hetts, Mark Wilson, Alastair Martin, and Susan Noworolski, for providing guidance and feedback these past few months. I would also like to thank the members of the Interventional Radiology Lab at China Basin, including Bridget Kilbride, Dr. Hee Jeung Oh, Parth Kumar, Teri Moore, Colin Yee, and Jack Williams, for creating an amazing atmosphere to work in and troubleshooting issues alongside me. A special thank you to Dr. Nancy Hills for her helpful advice on how to best analyze my data. Lastly, thank you to my peers in the MSBI program for an unforgettable and transformative year, and most importantly, to my family for always supporting me.

## Drug capture efficacy using polystyrenesulfonate-coated chemofilter device

Emilie Decavel-Bueff

### **Abstract**

Endovascular chemotherapy is an effective treatment option for cancer, however, the therapeutic agents used in this procedure often travel to non-target tissues and cause severe toxicity. Side-effects of chemotherapy range from nausea to life-threatening conditions. A strategy to reduce exposure of healthy tissues and organs to the toxicity of chemotherapeutic agents, such as doxorubicin (DOX), is to remove these drugs from systemic circulation after they have passed through the tumor site. With this goal in mind, different types of ChemoFilter devices have shown promise in alleviating these detrimental side effects. When placed downstream from the targeted tumor during intra-arterial chemotherapy, excess therapeutic agents bind to the device, preventing them from entering systemic circulation. In this study, we evaluated the doxorubicin-binding efficacy of a 3D printed porous cylindrical ChemoFilter device coated with sulfonated pentablock copolymers. Closed-circuit flow models experiments integrating 11 devices (uncoated or coated) at two concentrations of DOX (0.01 mg/mL and 0.05 mg/mL) were conducted. Samples collected from these flow models were used to treat H9c2 cell cultures, a rat embryonic cardiac cell line selected due to DOX cardiotoxicity. After a 24-hour treatment period, cell viability was calculated using the Trypan blue exclusion method. At 0.01 mg/mL DOX and 0.05 mg/mL DOX, the 3D printed polystyrenesulfonate-coated absorbers effectively filtered and eliminated DOX toxicity, increasing the H9c2 cell viability by 12.97% and 23.11%, respectively. These results confirm the ChemoFilter's ability to successfully absorb DOX *in vitro*, showing promise for its possible future use in clinical trials.

## Table of Contents

Introduction.....	1
Materials and Methods.....	5
Results.....	11
Discussion and Conclusion.....	18
References.....	24

## List of Figures

Figure 1. Concept for drug capture in blood vessel using two 3D printed polystyrenesulfonate-coated absorbers in parallel.....	2
Figure 2. Placement of filtration device (absorber) downstream of liver tumor site during an intra-arterial chemotherapy procedure. ....	3
Figure 3. Chemical structures of doxorubicin in its uncharged (A) and protonated (B) form, and the negatively charged sulfonate that coats the 3D printed absorber (C).....	3
Figure 4. <i>In vitro</i> closed-circuit flow model.....	6
Figure 5. One of the nine squares within the 3×3 grid of the hemocytometer after 24-hour treatment with (A) 89.75 μM of doxorubicin and with (B) PBS (Negative Control).....	9
Figure 6. Plating of HeLa cells at different volumes (3 mL, 2 mL, and 1.5 mL) and treated with or without 0.05 mg/mL DOX.....	11
Figure 7. Plating of HeLa cells at 2 mL and treated with or without 0.05 mg/mL DOX.....	11
Figure 8. Doxorubicin-induced morphological alterations in H9c2 cells at 0.01 mg/mL DOX.....	12
Figure 9. Effects of doxorubicin-induced cytotoxicity in H9c2 cell density at 0.01 mg/mL DOX.....	13
Figure 10. H9c2 cell cytotoxicity under the four conditions at 0.01 mg/mL DOX.....	14
Figure 11. Doxorubicin-induced morphological alterations in H9c2 cells at 0.05 mg/mL DOX.....	15
Figure 12. Effects of doxorubicin-induced cytotoxicity in H9c2 cell density at 0.05 mg/mL DOX.....	16
Figure 13. H9c2 cell cytotoxicity under the four conditions at 0.05 mg/mL of doxorubicin.....	17

## Introduction

Since 1991, overall cancer prognosis and survival have increased due to substantial developments made in early diagnosis and treatment strategies, with death rates declining by 27%<sup>1</sup>. However, according to the World Health Organization, cancer was still the second leading cause of death in 2018, killing roughly 9.6 million individuals globally<sup>2</sup>. Most notably, the number of cases of liver cancer have more than tripled in the last few decades in the US alone<sup>1</sup>. In fact, hepatocellular carcinoma (HCC), the most common type of primary liver cancer, is the third most common cause of cancer-related mortality worldwide<sup>3</sup>. This is predominantly observed among men, and even more so among those who are less educated<sup>4</sup>.

There are many treatment options available for HCC, including radiofrequency ablation, surgical resection, radiation therapy, and trans-arterial procedures<sup>5</sup>. Although liver transplantation is the most curative approach for HCC, recurrence rates remain high and less than 20% of patients qualify for surgery<sup>5,6</sup>. Due to strict patient eligibility criteria and to the shortage of donors, transplantation is not a viable option for many patients<sup>7</sup>. Instead, the standard of care for inoperable intermediate-stage HCC is trans-arterial intervention, including trans-arterial chemoembolization (TACE) and intra-arterial chemotherapy (IAC)<sup>7</sup>. Both are fluoroscopy-guided, minimally invasive procedures that use a catheter to deliver the chemotherapeutic agents directly to the tumor. While this targeted therapy approach does allow for more of the anti-cancer drug to reach the tumor, especially in comparison to conventional intra-venous chemotherapy, administered dose is still limited by severe side-effects. More than 50% of the injected drug travels past the tumor and enters circulation, affecting non-target tissues and causing systemic toxicity<sup>8</sup>.



In particular, doxorubicin (DOX), an anthracycline antibiotic widely used in the treatment of numerous solid organ cancers and commonly selected for HCC trans-arterial procedures, can be detrimental and potentially fatal to the patient<sup>9,10</sup>. Doxorubicin side effects include alopecia, neutropenia, mucositis, pericarditis, cardiomyopathy, left ventricular dysfunction, and congestive heart failure<sup>11,12</sup>. Despite this overwhelming limitation, studies have shown that increasing the dose of doxorubicin results in greater tumor suppression<sup>8,13</sup>. Thus, it is vital to find an effective method that would reduce the cardiotoxicity caused by doxorubicin while maintaining, or even improving, its clinical use as an anti-cancer drug.

A promising solution to reduce systemic toxicity is to incorporate a ChemoFilter device downstream of the tumor treatment site that would remove the excess drug before it enters general circulation (Figure 1). This could be implemented during an IAC procedure, as shown in

Figure 2. An introducer sheath and guidewire would be used to temporarily place the filtration device in the hepatic veins draining the liver. After doxorubicin is infused into the hepatic artery, the

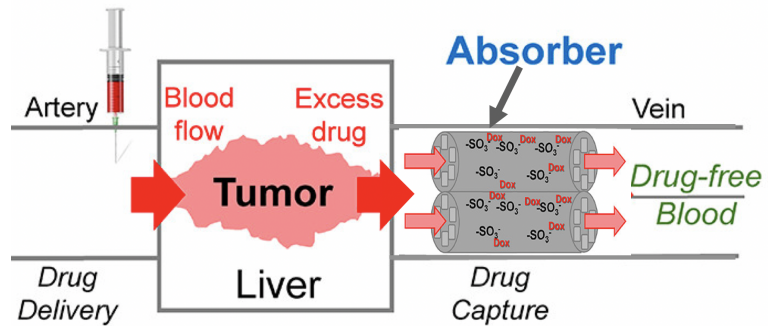


**Figure 1.** Concept for drug capture in blood vessel using two 3D printed polystyrenesulfonate-coated absorbers in parallel<sup>17</sup>.

drug would travel to the tumor, exit the liver, and be absorbed by the ChemoFilter before entering systemic circulation. Past studies have explored various binding methods that effectively filter doxorubicin and cisplatin from the bloodstream, such as sulfonated ion-exchange resins, DNA, and magnets<sup>14-16</sup>.

For the purpose of this study, we assessed a 3D printed polystyrenesulfonate-coated absorber designed by Dr. Hee Jeung Oh. At physiological pH, doxorubicin's amino functional group becomes protonated, giving the molecule an overall positive charge and a high affinity for anionic sulfonate groups (Figure 3). Electrostatic interactions between the positively charged nitrogen and negatively charged oxygen form an ionic bond and the sulfonate-coated absorber is able to bind to doxorubicin in blood. The device's drug capturing efficiency has been demonstrated *in vivo* using swine models, with up to  $64 \pm 6\%$  of doxorubicin successfully removed from circulation<sup>17</sup>.

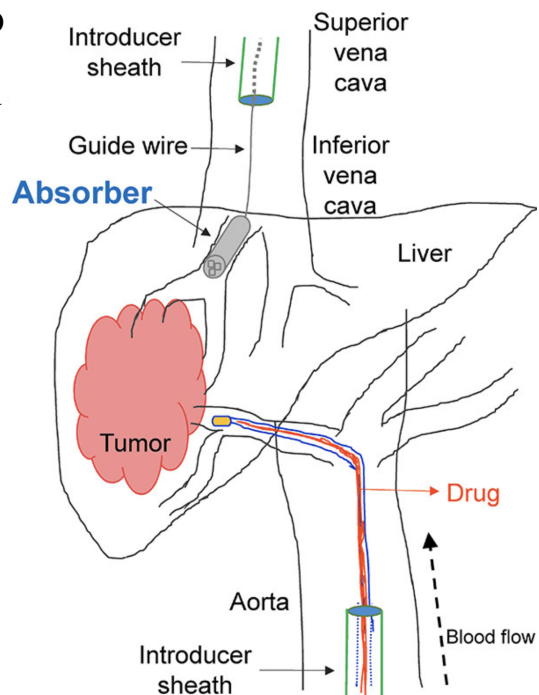


**Figure 2.** Placement of filtration device (absorber) downstream of liver tumor site during an intra-arterial chemotherapy procedure<sup>17</sup>.

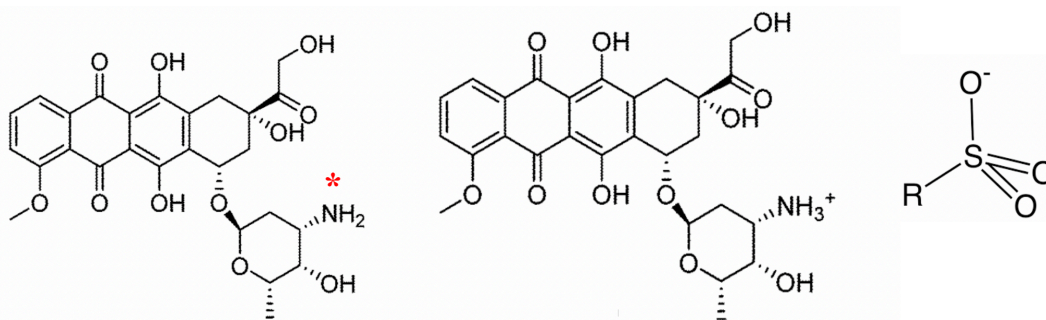


**Figure 3.** Chemical structures of doxorubicin in its uncharged (A) and protonated (B) form, and the negatively charged sulfonate that coats the 3D printed absorber (C). When doxorubicin is *in vivo* (pH 7.4), the nitrogen marked by an asterisk (A) becomes positively charged (B) and binds to the anionic oxygen in the sulfonate group (C).

In our study, we evaluated *in vitro* the doxorubicin drug-binding efficacy of this 3D printed porous cylindrical filtration device coated with sulfonated pentablock copolymers. Our investigation aimed to confirm the filter's ability to absorb doxorubicin, and therefore reduce systemic toxicity, as well as supplement data still currently being collected in *in vivo* studies.

Due to the prevalence and importance of doxorubicin-induced cardiotoxicity, the H9c2 rat cardiac cell line was selected for our cultures. This cell line was originally derived from embryonic BDIX rat heart tissue by Kimes and Brandt in 1976, and is a well-established model of myocardium that has been historically used to evaluate the cardiotoxicity caused by anticancer drugs, including doxorubicin<sup>18-20</sup>.

## Materials and Methods

Although our present study of doxorubicin toxicity in cell cultures focuses on H9c2 cells, the immortal HeLa cell line was first used to become familiar with and to optimize cell culture protocols for the H9c2 cell line. Then, to assess the ChemoFilter's ability to bind to doxorubicin and the residual toxicity to cardiac cells *in vitro*, samples taken from closed-circuit flow models with either uncoated or coated absorbers at different DOX concentrations were used to treat H9c2 cell cultures in toxicity experiments. After a 24-hour treatment period, percent cell viability was calculated to evaluate the filter's drug-binding efficacy and DOX cardiotoxicity.

### *Materials and Chemicals*

The porous cylinders of the absorbers were printed at Carbon, Inc (Redwood City, CA, USA). Dulbecco's Modified Eagle's Medium (DMEM), H9c2 cell line, 12-well cell culture plates, Steriflip vacuum filter, and bright line hemocytometer were purchased from Sigma-Aldrich (St.Louis, MO, USA). Penicillin Streptomycin (10,000 units/mL), sterile Phosphate Buffered Saline (PBS) pH 7.4 (1X), and 0.05% Trypsin-EDTA 1X were procured from Gibco Life Technologies Corporation (Grand Island, NY, USA). Dimethyl Sulfoxide (DMSO) and 6-well cell culture plates were purchased from Fisher Scientific (Hampton, NH, USA). Fetal Bovine Serum (FBS) was obtained from HyClone Laboratories (South Logan, UT, USA), DNase I from STEMCELL Technologies (Vancouver, BC, CA), 0.4% Trypan blue Solution with 0.85% NaCl from Lonza (Walkersville, MD, USA), CytoOne T-75 tissue culture flasks from USA Scientific (Ocala, FL, USA), and doxorubicin hydrochloride (2 mg/mL) from United States Pharmacopeia (New York, NY, USA). Serological pipets, micropipette tips, and conical tubes (50 mL and 15 mL) were obtained from Corning (Corning, NY, USA). NIS-Elements Advanced Research software was used to take images on the Nikon Eclipse TE2000-E inverted phase

contrast microscope, and the AmLite software was used to capture images on the Nikon Eclipse TS100 with the AMScope MU Series camera attachment. Images were processed and adjusted on ImageJ 2.

### *Flow Model Experiments*

In order to simulate intra-arterial delivery of chemotherapy agents and their capture by a specialized ChemoFilter device, an *in vitro* closed-circuit flow model was developed by Patel and colleagues (Figure 4)<sup>21</sup>. This model used polyvinyl chloride tubing with a diameter similar to that of the human hepatic vein (1.2 cm) and a peristaltic pump to maintain a constant flow rate to match human hepatic blood flow (750 mL/min). Two different concentrations of doxorubicin

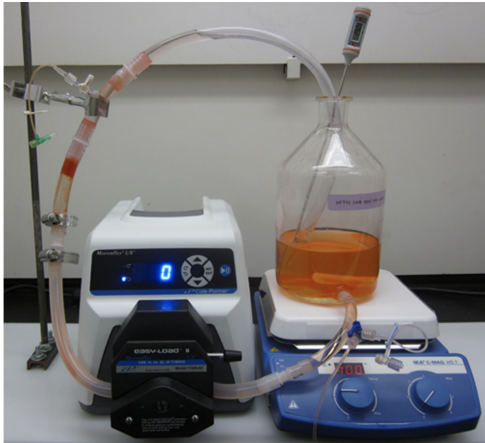


**Figure 4.** *In vitro* closed-circuit flow model<sup>21</sup>.

were tested: 0.01 mg/mL and 0.05 mg/mL in 500 mL of PBS, which was heated to 37°C. These dosages are within the range of concentrations that have been used in clinical TACE procedures<sup>22</sup>. Flow models at each of the described doxorubicin concentrations were performed using 11 coated (experimental) or uncoated (control)

filtration devices inserted within the tubing. For the

uncoated filters, up to 2 mL samples were taken at time point zero. For the coated devices, 2 mL samples were collected after equilibrium had been reached in the system. This occurred at hour 2 for the 0.01 mg/mL concentration and at hour 6 for the 0.05 mg/mL concentration. These samples represent the amount of systemic doxorubicin in circulation following chemotherapy treatment. All samples were then filter-sterilized and used to treat H9c2 cell cultures to assess toxicity.

### *HeLa Cell Cultures*

The HeLa cell line is derived from human cervical epithelial carcinoma<sup>23</sup>. The HeLa cells were cultured in high glucose (4.5 g/L) DMEM supplemented with antibiotics (100 units/mL penicillin and 100 µg/mL streptomycin) and 10% FBS at 37°C in a humidified atmosphere of 5% CO<sub>2</sub>. Every 2-3 days, cells reached 90% confluence and were treated with 0.05% trypsin/EDTA solution in order to detach the cells from the flask surface on which they adhered. The collected cells were then centrifuged (200×g for 5-10 min at 22°C). The cell pellets were resuspended in 10 mL of fresh, complete media and subcultured into 75-cm<sup>2</sup> flasks at a ratio of 1:2, with each flask containing 5 mL of cell suspension.

Cells were seeded into 6-well tissue culture plates to explore optimal seeding conditions. Both the ideal ratio of cell suspension to media and the total volume of cell suspension per well were evaluated. Dilution of cell suspension in complete media consisted of 1:5, 1:2, 1:1, 2:1, and 5:1 (3 mL total volume), and volumes tested were 3 mL, 2 mL, and 1.5 mL (1:1 dilution only). Each test volume was also treated with or without doxorubicin (0.05 mg/mL) for 24 hours immediately after plating. Images were acquired every two hours for eight hours, and a final image was captured at 24 hours.

### *H9c2 (2-1) Cell Cultures*

The H9c2 cell line was grown in 75-cm<sup>2</sup> tissue culture flasks in high glucose (4.5 g/L) DMEM containing 10% FBS and antibiotics (100 units/mL penicillin and 100 µg/mL streptomycin) and incubated in a humidified atmosphere of 5% CO<sub>2</sub> at 37°C. Culture medium was replaced every 2-3 days, and the cells were subcultured at 70-80% confluence to maintain their proliferative, undifferentiated state. Upon reaching confluency, cells were rinsed twice with sterile PBS to remove residual medium, and they were then temporarily incubated in 0.05%

trypsin/EDTA solution. When 90% of the cells were dissociated, medium was added to inhibit trypsin activity. The resulting suspension of cells was centrifuged at  $120 \times g$  ( $4^{\circ}\text{C}$ ) for 5 minutes and the cell pellet was resuspended in 5 mL of fresh medium. To ensure the correct seeding density of  $1 \times 10^4$  cells/cm<sup>2</sup> during passaging and plating, Trypan blue and a hemocytometer were used to calculate cell density. To reduce clumping caused by prolonged treatment with trypsin, cells of passage 8 were incubated in DNase I for 15 minutes at room temperature. For passages 4, 7 through 12, and 15, an aliquot of cells was frozen in a freezing medium made of 10% DMSO and 90% FBS. This allowed for re-culturing of cells from earlier passages to repeat experiments, if needed.

#### *Toxicity Study Protocol*

H9c2 cells were seeded ( $\sim 35,000$  cells/mL) into 6-well plates with a total cell suspension volume of 2 mL per well, or into 12-well plates with a total cell suspension volume of 800  $\mu\text{L}$  per well. For each toxicity experiment, cells were divided into nine treatment groups ( $n=3$ ): a Negative Control (PBS only) and four different conditions for each initial concentration of doxorubicin (0.01 mg/mL and 0.05 mg/mL):

1. **Coated Filter** — samples taken from the flow model integrating coated absorbers
2. **Uncoated Filter** — samples taken from the flow model integrating uncoated absorbers
3. **0.45  $\mu\text{M}$  or 2.24  $\mu\text{M}$**  — stock solution of doxorubicin (2 mg/mL) diluted in PBS at the concentrations indicated above prior to treating cell cultures
4. **18.31  $\mu\text{M}$  or 89.75  $\mu\text{M}$**  — stock solution of doxorubicin used to acquire *final* concentration (0.01 mg/mL or 0.05 mg/mL) within each well after treatment

All cell culture plates were incubated in a humidified atmosphere of 5%  $\text{CO}_2$  at  $37^{\circ}\text{C}$  for 24 hours to facilitate adhesion. After attachment, 50  $\mu\text{L}$  (for the 6-well plates) or 20  $\mu\text{L}$  (for the 12-

well plates) of the appropriate treatment was introduced to each well and left for an additional 24-hour period. These incubation and treatment periods of 24 hours are commonly used in cytotoxicity studies in this cell line<sup>24-28</sup>.

Every 2-6 hours during the treatment period, cells were observed through a Nikon Eclipse TE2000-E inverted phase contrast microscope to evaluate their morphological changes over time, obtain preliminary cell counts, and capture images. To ensure that the same center location of each well was consistently used for cell counting, reference marks were drawn on a paper placed under the cell culture plates. Additional images were taken 24 and 48 hours after incubation on the Nikon Eclipse TS100 using the MU Series camera attachment. Trypan blue was used to obtain accurate counts of live and dead cells at the end of the 24-hour treatment period.

### *Cell Counting*

H9c2 cell viability was determined using the Trypan blue exclusion method. This dye penetrates dead cells through damaged membranes and stains them blue, while live cells remain

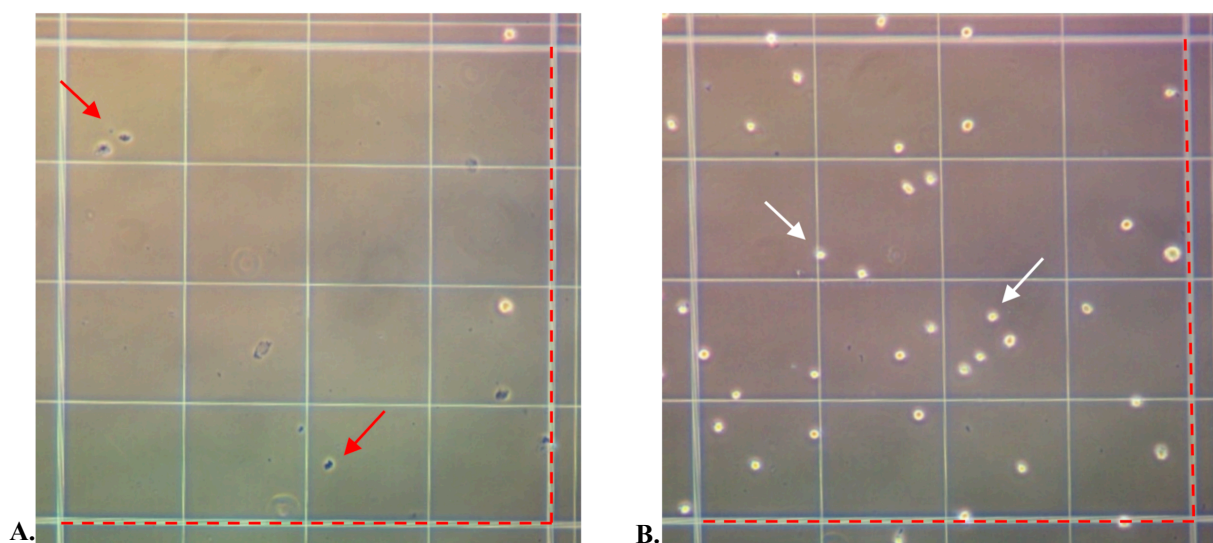


**Figure 5.** One of the nine squares within the 3×3 grid of the hemocytometer after 24-hour treatment with (A) 89.75  $\mu\text{M}$  of doxorubicin and with (B) PBS (Negative Control). White arrows point to live cells while red arrows point to dead cells. Exclusion lines are in red.



colorless (Figure 5). Unadhered dead cells in the medium were included in the cell count. After the removal of the medium into a 15 mL centrifuge tube, adherent viable cells were rinsed twice with PBS before trypsinization. The cell pellet was then resuspended in 2 mL (for 6 well-plates) or 200  $\mu$ L (for 12 well-plates) of complete medium, and a 50  $\mu$ L aliquot was removed and diluted with 50  $\mu$ L of 0.4% Trypan blue solution. 10  $\mu$ L of that solution was pipetted to the hemocytometer and the 3  $\times$  3 grid was visualized under a Nikon Eclipse TS100 with a 10x objective. The number of live and dead cells within all nine squares was counted and those touching the right or bottom boundaries were excluded. The following calculations were performed:

$$\text{Percent Viability} = \frac{\text{No. of Viable Cells}}{\text{Total No. of Cells}} \times 100\%$$

$$\text{Concentration of Viable Cells} = \frac{\text{No. of Viable Cells}}{\text{No. of Squares}} \times 2 (\text{Dilution Factor}) \times \frac{1 \text{ Square}}{10^{-4} \text{ mL of Cell Suspension}}$$

### *Statistical Analysis*

Results from 2 independent experiments with triplicates are presented as mean  $\pm$  standard error of the mean (SEM). Statistical analysis was performed using RStudio. Data was analyzed using one-way analysis of variance (ANOVA) followed by Tukey *post hoc* test. Statistical differences were considered significant when  $p < 0.05$ .

## Results

### *HeLa Cell Cytotoxicity*

For all volumes of cell suspension, HeLa cells never adhered at any time points and all cells were dead and floating in the solution when treated with 0.05 mg/mL of doxorubicin (Figure 6). Density of adherent cells increased with increasing volume when cells were not treated with doxorubicin for 24 hours, with cell density below optimal in 1.5 mL and cells almost at 100% confluency in 3 mL of cell suspension. Similar cell structures and clumping patterns were

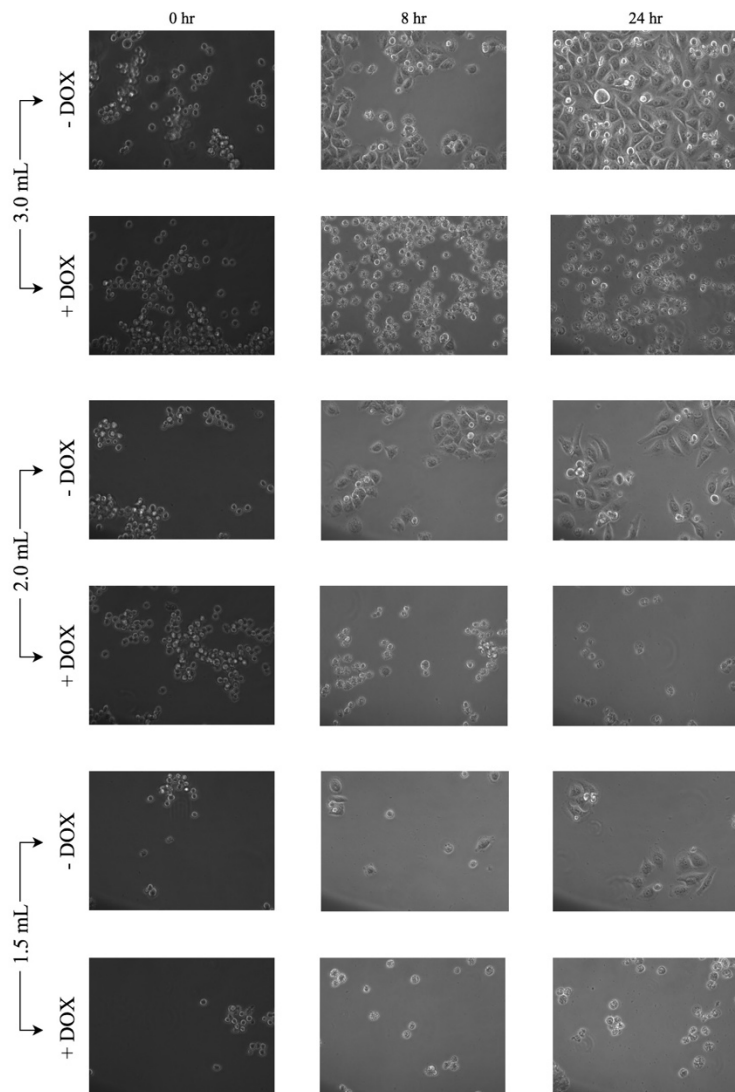


**Figure 6.** Plating of HeLa cells at different volumes (3 mL, 2 mL, and 1.5 mL) and treated with (+) or without (-) 0.05 mg/mL DOX. Images taken at time points 0, 8, and 24 hr after the start of treatment.

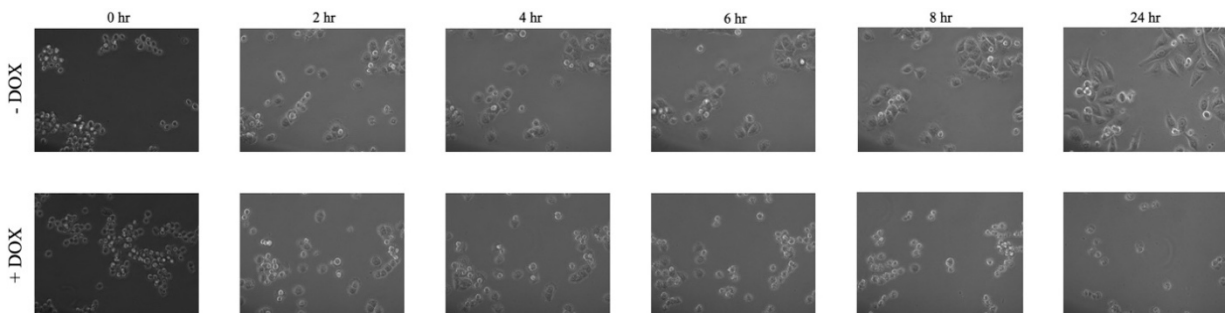


**Figure 7.** Plating of HeLa cells at 2 mL and treated with (+) or without (-) 0.05 mg/mL DOX. Images taken at time points 0, 2, 4, 6, 8, and 24 hours and at the same location within the wells.

identified in the images taken over time, confirming that the same area in the center of the wells was captured (Figure 7).

### *H9c2 Cell Viability at 0.01 mg/mL DOX*

After incubating for 24 hours, H9c2 cells were adhered to the surface of the wells (Figure 8). All adhered cells at this time point were flat and spindle-shaped, with a few rounded, brighter cells that were only partially adhered. Such cells were fully attached to the surface within three

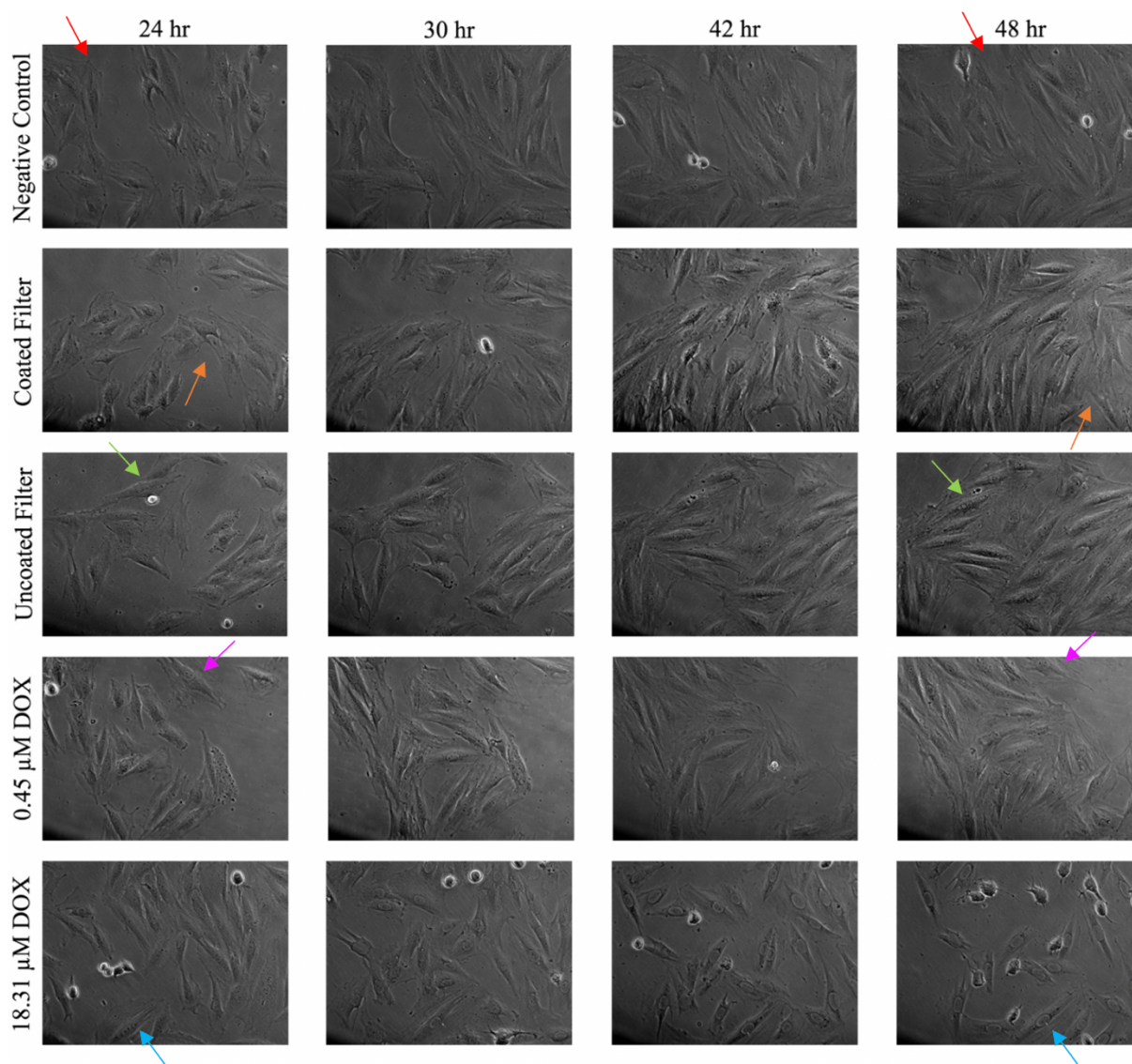


**Figure 8.** Doxorubicin-induced morphological alterations in H9c2 cells with 20x objective under the Nikon Eclipse TE2000-E inverted microscope. Initial DOX concentration for the flow model samples (Coated Filter and Uncoated Filter) was 0.01 mg/mL DOX. Images taken at the same location within the wells right before treatment (24 hr), and 6, 18, and 24 hours after treatment. Arrows of similar colors point to identical structures observed over time.

hours. As time progressed, cell density increased in most treatment conditions, except for 18.31  $\mu\text{M}$  DOX. This trend was more pronounced in the Negative Control, the Coated Filter, and the Uncoated Filter conditions. With higher densities, cells began to organize themselves into more

orderly arrays, which was most

evident in the Coated Filter at

48 hr. Reduction in cell size

and number was clearer when

treated with 18.31  $\mu\text{M}$  DOX.

Within the cells, deterioration

started at the periphery and

progressed inwards. Compared

to the Negative Control, the

nuclear size in 18.31  $\mu\text{M}$  DOX

increased slightly.

Additionally, more partially

adhered cells were visible in

18.31  $\mu\text{M}$  DOX at time 48 hr

than at any other time point or

for any other treatment

condition. Such cells are more

likely to be detaching than

adhering.

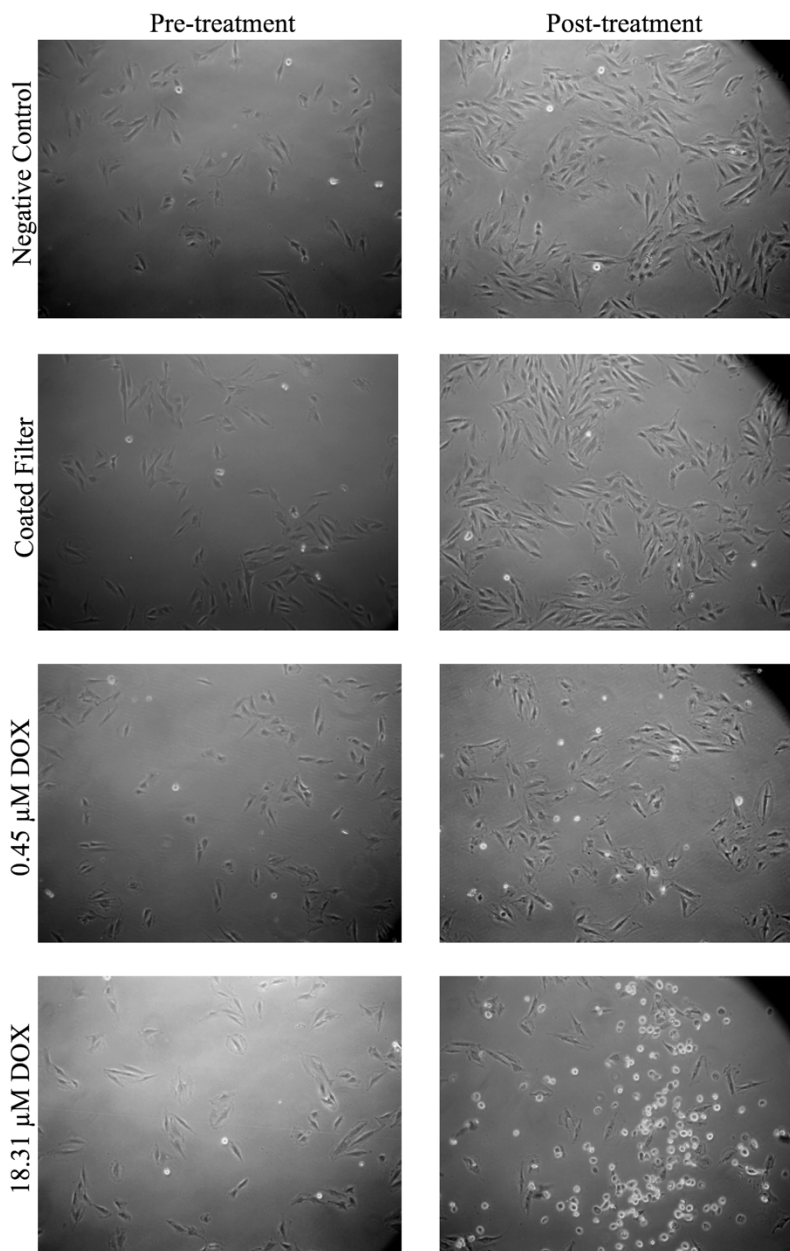


**Figure 9.** Effects of doxorubicin-induced cytotoxicity in H9c2 cell density. Images were taken pre-treatment (24 hours after plating) and post-treatment (48 hours after plating) under the Nikon Eclipse TS100 microscope with 10x objective. Flow model DOX concentration for Coated Filter was 0.01 mg/mL.

Similar low cell densities, with cells randomly orienting themselves with respect to each other, were achieved for each condition before 0.01 mg/mL DOX treatments were introduced to the wells (Figure 9). After the 24-hour treatment period, the density of live cells in the Negative Control and Coated Filter conditions was comparable. While there were more unadhered dead cells at 0.45  $\mu$ M DOX compared to the Coated Filter, the most obvious difference between those two conditions was a clear reduction in adhered live cells. These differences were even more pronounced in 18.31  $\mu$ M DOX, which exhibited an abundance of floating cells and very few cells adhered to the well surface.

For the treatment concentration of 0.01 mg/mL, H9c2 cell survival was significantly reduced when treated with 18.31  $\mu$ M DOX, 0.45  $\mu$ M DOX, and Uncoated Filter for 24 hours (Figure 10). Compared to Negative Control, cell viability decreased by 34.23% in 18.31  $\mu$ M DOX and 12.53% in the Uncoated Filter. No statistical significance was found between 0.45  $\mu$ M

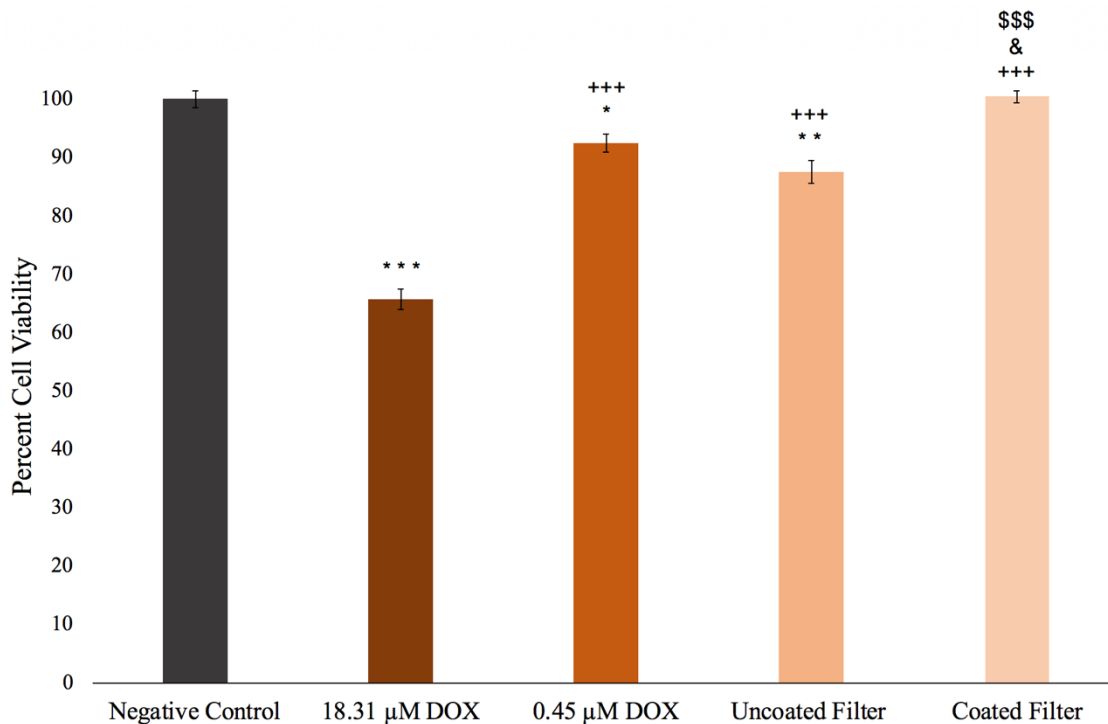


**Figure 10.** H9c2 cell cytotoxicity under the four conditions at 0.01 mg/mL of doxorubicin after 24 hours of treatment. Data presented as the mean percentage of cell viability relative to the Negative Control (\* $p < 0.05$ , \*\* $p < 0.0005$ , \*\*\* $p < 0.0001$  vs. Negative Control; +++ $p < 0.0001$  vs. 18.31  $\mu$ M DOX; & $p < 0.05$  vs. 0.45  $\mu$ M DOX; \$\$\$ $p < 0.0001$  vs. Uncoated Filter).

DOX and Uncoated Filter, or between the Negative Control and Coated Filter. However, cell viability did significantly increase by 12.97% from the Uncoated to Coated Filter.

### *H9c2 Cell Viability at 0.05 mg/mL DOX*

As observed in the 0.01 mg/mL DOX treatments, almost all cells were fully adhered to the surface of the wells after 24 hours of incubation (Figure 11). Most adhered cells were flat and spindle-shaped, and only two rounded, partially adhered cells were visible. As time progressed,

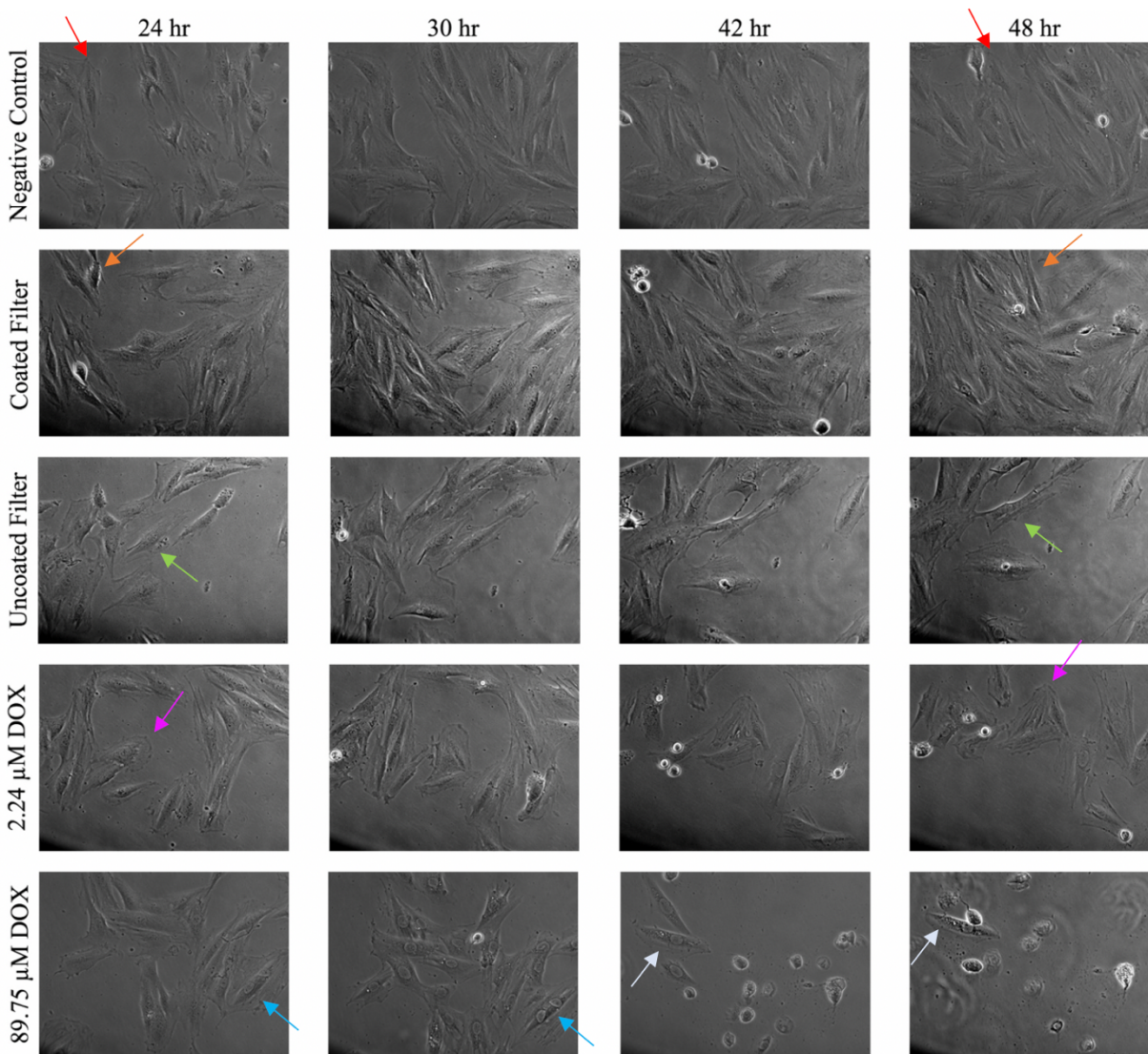


**Figure 11.** Doxorubicin-induced morphological alterations in H9c2 cells with 20x objective under the Nikon Eclipse TE2000-E inverted microscope. Initial DOX concentration for the flow model samples (Coated Filter and Uncoated Filter) was 0.05 mg/mL DOX. Images taken at the same location within the wells right before treatment (24 hr), and 6, 18, and 24 hours after treatment. Arrows of similar colors point to identical structures observed over time.

cell density increased in the Negative Control and the Coated Filter, while density decreased in the other treatment conditions. Notably, at the end of the treatment period, cells treated with 2.24  $\mu\text{M}$  DOX and Uncoated Filter had the same number of adherent cells. Similar trends in deterioration of cell structure and number observed at 0.01 mg/mL DOX were seen here at 0.05 mg/mL DOX, with the addition of cytoplasmic vacuolization that started to develop as early as 3 hours after treatment. At 48 hr 89.75  $\mu\text{M}$  DOX, only one adhered, spindle-shaped cell was detected and many floating cells were out of focus. There were more cellular debris in 89.75  $\mu\text{M}$  DOX, at 21 hr and 48 hr.

Again, essentially identical cell densities were achieved for each condition before 0.05 mg/mL DOX treatments began (Figure 12). After cells were treated for 24 hours, the density of live cells between the Negative Control

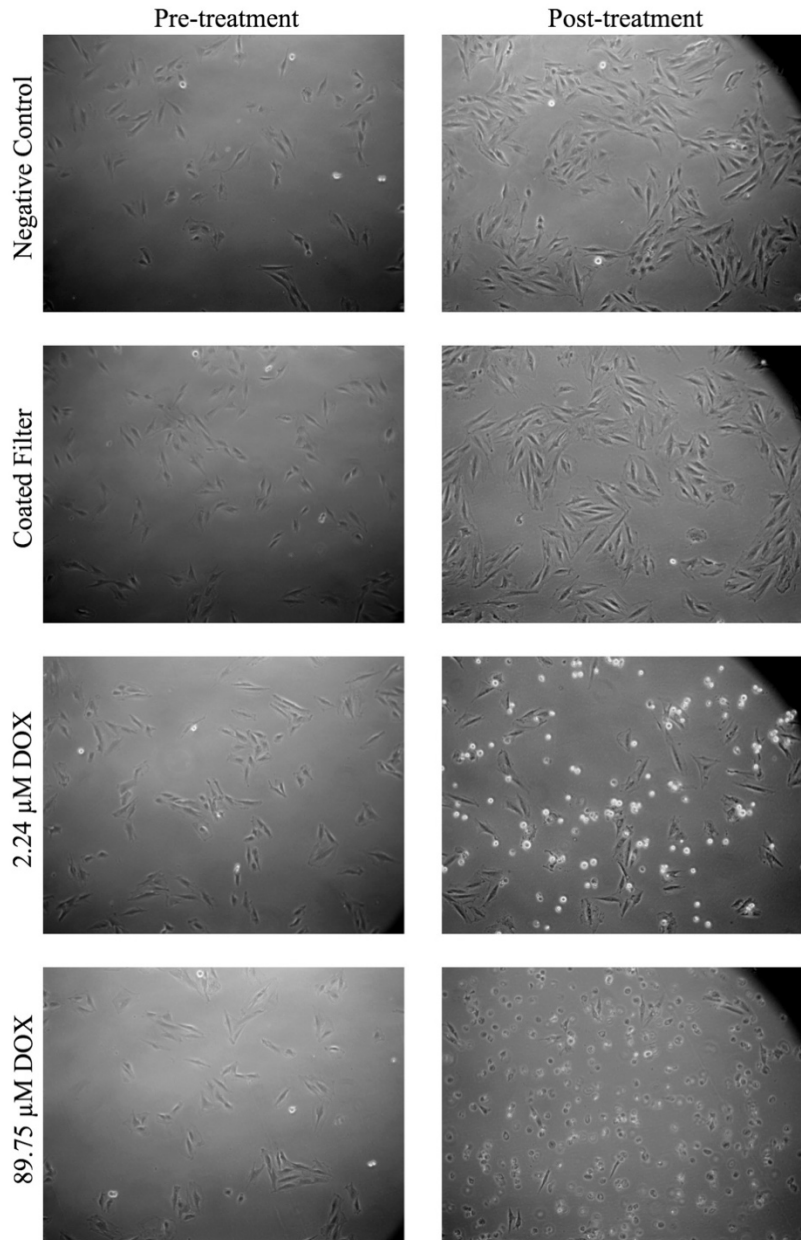


**Figure 12.** Effects of doxorubicin-induced cytotoxicity in H9c2 cell density. Images were taken pre-treatment (24 hours after plating) and post-treatment (48 hours after plating) under the Nikon Eclipse TS100 microscope with 10x objective. Flow model DOX concentration for Coated Filter was 0.05 mg/mL.

and Coated Filter was comparable. In 2.24  $\mu\text{M}$  DOX, post treatment, more unadhered dead cells were observed with fewer viable cells adhered to the surface of the well. At 89.75  $\mu\text{M}$  DOX, only a handful of adhered cells could be seen under the dense population of floating dead cells.

H9c2 cell survival was significantly reduced when treated with 89.75  $\mu\text{M}$  DOX, 2.24  $\mu\text{M}$  DOX and Uncoated Filter at 0.05 mg/mL for 24 hours (Figure 13). At that concentration, compared to the Negative Control, cell viability decreased by 69.95% in 89.75  $\mu\text{M}$  DOX, and by 24.45% in Uncoated Filter. No statistical significance was found between 2.24  $\mu\text{M}$  DOX and Uncoated Filter, or between the Negative Control and Coated Filter. However, cell viability did significantly increase by 23.11% from the Uncoated to Coated Filter.

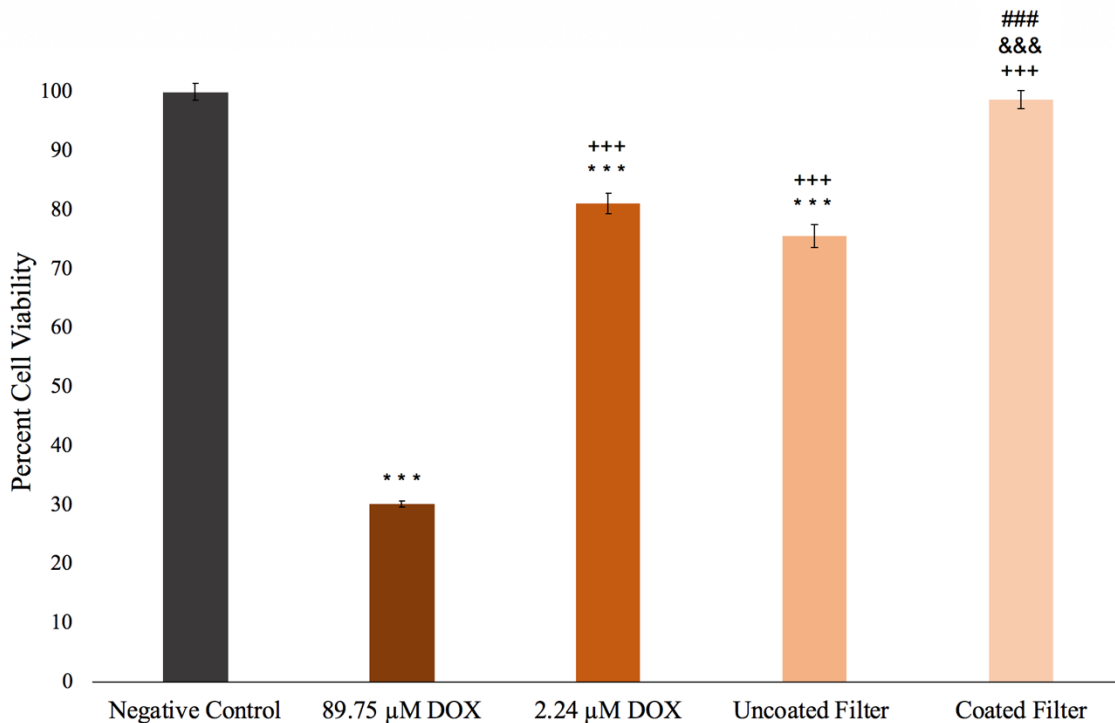


**Figure 13.** H9c2 cell cytotoxicity under the four conditions at 0.05 mg/mL of doxorubicin after 24 hours of treatment. Data presented as the mean percentage of cell viability relative to the Negative Control (\*\*p < 0.0001 vs. Negative Control; +++p < 0.0001 vs. 89.75  $\mu\text{M}$  DOX; &&&p < 0.0001 vs. 2.24  $\mu\text{M}$  DOX; ###p < 0.0001 vs. Uncoated Filter).



## Discussion and Conclusion

The aim of this study was to assess the doxorubicin drug-binding efficiency of the 3D printed polystyrenesulfonate-coated absorber. This was done by conducting flow model experiments integrating the device (uncoated or coated) at the two concentrations of doxorubicin (0.01 mg/mL and 0.05 mg/mL). H9c2 cell cultures were treated with the supernatants collected from the described flow models, and the resulting cell viability was calculated after 24 hours of treatment. The coated device successfully absorbed significantly more doxorubicin than the uncoated filters at both concentrations, resulting in H9c2 cell viability similar to the Negative Control. These results confirmed the efficacy of the absorber *in vitro* and will help pave the way to implement the devices in clinical human studies.

### *HeLa Cell Cytotoxicity*

The HeLa cell line has been used to study the effects of toxic agents, such as nitrogen doped carbon quantum dots, nickel nanotubes, and the proteasome inhibitor epoxomicin<sup>29-31</sup>. Our preliminary study conducted on HeLa cells aided in establishing and optimizing an effective experimental protocol for the H9c2 cell line. The lack of adherent cells at any time points after doxorubicin treatment revealed that an incubation period for the H9c2 cells would be necessary (Figure 6). This would give viable cells adequate time to adhere to the surface prior to treatment so that the cellular damage caused by the chemotherapeutic agent could be evaluated. Additionally, allowing the healthy cells to adjust and grow into their normal morphology is a more clinically relevant representation of *in vivo* conditions. Based on the images acquired from the HeLa cell line experiments, a dilution factor of 2 and a plating volume of 2 mL achieved the optimal seeding density to best visualize individual cells over time (Figure 6). When HeLa cells were incubated without doxorubicin, they remained adhered to the well surface and continued to

spread by webbing: extending lamellipodia and filopodia with protoplasm filling the space in between (Figure 7)<sup>32</sup>. In sharp contrast, cells treated with the drug were exclusively round in shape and free-floating. Similar results were expected for the application on H9c2 cells. Due to the prevalence of cardiotoxicity induced by doxorubicin, we used this cell line of rat cardiomyoblasts for the remainder of our study.

### *H9c2 Cell Cardiotoxicity*

H9c2 cardiomyoblast cells grown in culture dishes can be categorized into three subgroups: adherent, sub-adherent, and non-adherent. Typically, if cells have not started to adhere to the surface of the dishes within 24 hours of plating, then they were considered dead. Examples of these rounded, floating, and brighter cells can be seen in Figures 9 and 12 (Pre-treatment), which show images taken after the 24-hour incubation period. On the other hand, both adhered and partially adhered cells are considered live and can come in a variety of shapes: spherical, polygonal, and, more commonly, flat spindle-to stellate<sup>33</sup>. Most cardiomyoblasts are mononucleated and contain one to four nucleoli within their nuclei, a morphology which was generally observed within our H9c2 cell cultures<sup>18</sup>.

When H9c2 cells were incubated in doxorubicin, major structural changes occurred, including nuclear swelling, decrease in cell size, peripheral degeneration, membrane blebbing, and cell rounding (Figures 8 and 11). These morphological changes were more evident at higher DOX molar concentrations, with cytoplasmic vacuolization appearing at 89.75  $\mu$ M DOX, demonstrating the relationship between DOX dose and cytotoxicity. As cells were exposed to the drug over time, flat cells began to detach from the well surface, remaining only partially adhered through long cytoplasmic filopodia, until they were completely dissociated<sup>33</sup>. These observable changes are helpful in understanding how the chronic exposure to doxorubicin chemotherapy

affects cardiac cells. When looking at our images, it is important to note that the inconsistencies in cell density in response to treatment, such as the Uncoated Filter at 0.01 mg/mL DOX, are a consequence of the capture of a small area within the entire well using a 20x objective. Images taken using the 10x objective are more representative of how the population of cells were responding to DOX treatment. Within this larger field of view, we can clearly see that 89.75  $\mu$ M DOX and 2.24  $\mu$ M DOX were more fatal to H9c2 cells than the corresponding treatments at 0.01 mg/mL DOX (Figures 9 and 12). Given that there was no significant change in cell viability between the lower molar concentrations (0.45  $\mu$ M and 2.24  $\mu$ M DOX) and the corresponding Uncoated Filter, we are able to interpret the images similarly. For each DOX concentration in the flow models, the density of adherent cells in the Coated Filter and Negative Control were identical, which is also supported by the non-significant difference in the calculated cell viabilities for those treatments (Figures 10 and 13). The stark qualitative and numerical differences between Coated Filter and 0.45  $\mu$ M or 2.24  $\mu$ M DOX (also interpretable as Uncoated Filter) is reflective of the filter's drug-binding capabilities at both 0.01 mg/mL and 0.05 mg/mL DOX. This indicates that at each of the respective DOX concentrations, the 3D printed polystyrenesulfonate coated absorber is able to effectively eliminate DOX toxicity, allowing the cardiac myoblasts to thrive similarly to the Negative Control.

#### *Limitations and Future Directions*

In order to assess the cardiac cytotoxicity of doxorubicin, cell viability was calculated by utilizing the Trypan blue exclusion method. While live cells have intact cell membranes and exclude this dye, dead cells become stained blue due to their ruptured membranes<sup>34</sup>. Since the early 1900s, Trypan blue has been the gold standard for counting the number of live and dead cells in a variety of applications<sup>35,36</sup>. Such uses have included counting white blood cells in urine

sediments of dogs in veterinary pathological studies, and measuring the cytotoxicity of dibutyl phthalate on macrophages in immunopharmacology experiments<sup>37,38</sup>. Despite its extensive use in laboratory procedures, it has some limitations. Research has shown that Trypan blue is toxic to mammalian cells, often causing major and irreversible morphological changes within minutes of exposure. Tsaousis and colleagues found that the calculated cell viability of human trabecular meshwork cells decreased by 11% after only 5 minutes of exposure, and by 16% after 15 minutes<sup>39</sup>. To mitigate this issue, we counted H9c2 cells within 3 to 5 minutes of diluting the cell suspension with Trypan blue. Furthermore, while it is effective in staining the cytoplasm of dead cells, Trypan blue is not able to distinguish accurately between viable cells and cells that are alive, but dying<sup>40</sup>. A possible solution for this would be to assess cell viability by other means, such as the commonly used MTT colorimetric assay<sup>34</sup>. Instead of relying on the integrity of the cell membrane, this assay measures cell proliferation, or the quantity of cells that are actively dividing, and therefore is able to quantify the proportion of healthy cells in a population. Specifically, this assay measures the mitochondrial metabolic rate of active cells<sup>41</sup>. In the presence of these cells and through the action of dehydrogenase enzymes, the yellow tetrazolium salt 3-(4,5-Dimethylthiazol-2-yl)-2,5-diphenyltetrazolium bromide (MTT) is reduced to purple formazan crystals, which can then be dissolved and the optical density measured with a spectrophotometer<sup>42</sup>.

The flow model samples used in this study to treat H9c2 cells is another area that could be improved, specifically the final concentration of DOX in the cell cultures. The initial design of this study was to evaluate the drug-binding capabilities of the ChemoFilter device at two specific concentrations of doxorubicin (0.01 mg/mL and 0.05 mg/mL), concentrations selected due to their clinical use in chemotherapy, and then to treat the cell cultures with samples

acquired from the flow models<sup>43</sup>. However, since only a small aliquot of these samples (20  $\mu\text{L}$  or 50  $\mu\text{L}$ ) was transferred to the wells (initially containing 800  $\mu\text{L}$  or 2 mL of cell suspension), it was concluded that all flow model and samples of DOX stock solution with PBS were diluted by a factor of 40. In fact, only two treatments had a final concentration of 0.01 mg/mL or 0.05 mg/mL of doxorubicin within the wells: 18.31  $\mu\text{M}$  and 89.75  $\mu\text{M}$  DOX, respectively. On the other hand, the final molarity of doxorubicin for the samples that were diluted in PBS to acquire a concentration of 0.01 mg/mL or 0.05 mg/mL DOX prior to treating cell cultures was 0.45  $\mu\text{M}$  and 2.24  $\mu\text{M}$  DOX. Although the more diluted molar concentrations of doxorubicin have been used in similar H9c2 cardiotoxicity experiments, future studies could use DMEM as the solution in the flow models, instead of PBS<sup>44,45</sup>. Collected flow model samples could replace the medium in the H9c2 cell cultures, in which the final concentration would then reflect the true DOX concentration in the flow models.

A significant benefit of temporarily deploying a highly efficient absorber in patients during intra-arterial chemotherapy is the ability to increase the therapeutic dosage in order to maximize tumor suppression, resulting in better patient outcome and minimizing severe side effects. To that effect, future investigations could explore the upper limits of this absorber's capacity to filter doxorubicin. Determining at what concentration of doxorubicin the ChemoFilter would be able to successfully absorb enough of the drug and still result in a high percentage of cell viability in H9c2 cell cultures would provide valuable information in the future clinical use of these filtration devices.

In conclusion, the 3D printed porous cylindrical filtration device coated with sulfonated pentablock copolymers demonstrated successful binding and absorption of doxorubicin from circulation within a closed-circuit flow model. At 0.05 mg/mL and 0.01 mg/mL of DOX, the

absorber increased the H9c2 cell viability by 23.11% and 12.97%, respectively. With the results acquired in this *in vitro* study supporting the data currently being collected *in vivo*, the future clinical implications remain quite promising. Implementation of this ChemoFilter device would ultimately enhance the effectiveness of a standard intra-arterial chemotherapy procedure by significantly reducing systemic toxicity and improving patient prognosis. Application of these absorbers could be extended to treat other solid organ tumors in addition to hepatocellular carcinoma. Similar devices could also be adapted to selectively absorb other chemotherapeutics, such as cisplatin, carboplatin, and epirubicin, or to potentially filter antibiotics and other drugs.

## References

1. Facts & Figures 2019: US Cancer Death Rate has Dropped 27% in 25 Years. Available at: <https://www.cancer.org/latest-news/facts-and-figures-2019.html>. (Accessed: 29th August 2019)
2. Cancer. Available at: <https://www.who.int/news-room/fact-sheets/detail/cancer>. (Accessed: 29th August 2019)
3. Coskun, M. Hepatocellular Carcinoma in the Cirrhotic Liver: Evaluation Using Computed Tomography and Magnetic Resonance Imaging. *Exp. Clin. Transplant.* **15**, 36–44 (2017).
4. Ma, J., Siegel, R. L., Islami, F. & Jemal, A. Temporal trends in liver cancer mortality by educational attainment in the United States, 2000-2015. *Cancer* **125**, 2089–2098 (2019).
5. Kang, J.-K. *et al.* Stereotactic body radiation therapy for inoperable hepatocellular carcinoma as a local salvage treatment after incomplete transarterial chemoembolization. *Cancer* **118**, 5424–5431 (2012).
6. Schlachterman, A. Current and future treatments for hepatocellular carcinoma. *World Journal of Gastroenterology* **21**, 8478 (2015).
7. Raza, A. Hepatocellular carcinoma review: Current treatment, and evidence-based medicine. *World Journal of Gastroenterology* **20**, 4115 (2014).
8. Hwu, W. J. *et al.* A clinical-pharmacological evaluation of percutaneous isolated hepatic infusion of doxorubicin in patients with unresectable liver tumors. *Oncol. Res.* **11**, 529–537 (1999).
9. Marelli, L. *et al.* Transarterial therapy for hepatocellular carcinoma: which technique is more effective? A systematic review of cohort and randomized studies. *Cardiovasc. Intervent. Radiol.* **30**, 6–25 (2007).

10. Zhang, Y.-Y., Yi, M. & Huang, Y.-P. Oxymatrine Ameliorates Doxorubicin-Induced Cardiotoxicity in Rats. *Cellular Physiology and Biochemistry* **43**, 626–635 (2017).
11. Coufal, N. & Farnaes, L. Anthracyclines and Anthracenediones. *Cancer Management in Man: Chemotherapy, Biological Therapy, Hyperthermia and Supporting Measures* 87–102 (2011). doi:10.1007/978-90-481-9704-0\_5
12. Angsutararux, P., Luanpitpong, S. & Issaragrisil, S. Chemotherapy-Induced Cardiotoxicity: Overview of the Roles of Oxidative Stress. *Oxid. Med. Cell. Longev.* **2015**, 795602 (2015).
13. Porrata, L. F. & Adjei, A. A. The pharmacologic basis of high dose chemotherapy with haematopoietic stem cell support for solid tumours. *British Journal of Cancer* **85**, 484–489 (2001).
14. Patel, A. S. *et al.* Development and Validation of Endovascular Chemotherapy Filter Device for Removing High-Dose Doxorubicin: Preclinical Study. *J. Med. Device.* **8**, 0410081–0410088 (2014).
15. Aboian, M. S. *et al.* In vitro clearance of doxorubicin with a DNA-based filtration device designed for intravascular use with intra-arterial chemotherapy. *Biomed. Microdevices* **18**, 98 (2016).
16. Mabray, M. C. *et al.* In Vitro Capture of Small Ferrous Particles with a Magnetic Filtration Device Designed for Intravascular Use with Intraarterial Chemotherapy: Proof-of-Concept Study. *J. Vasc. Interv. Radiol.* **27**, 426–32.e1 (2016).
17. Oh, H. J. *et al.* 3D Printed Absorber for Capturing Chemotherapy Drugs before They Spread through the Body. *ACS Cent Sci* **5**, 419–427 (2019).
18. Kimes, B. W. & Brandt, B. L. Properties of a clonal muscle cell line from rat heart. *Exp. Cell Res.* **98**, 367–381 (1976).



19. Ma, J. *et al.* Rac1 signalling mediates doxorubicin-induced cardiotoxicity through both reactive oxygen species-dependent and -independent pathways. *Cardiovascular Research* **97**, 77–87 (2013).
20. Stěrba, M. *et al.* Oxidative stress, redox signaling, and metal chelation in anthracycline cardiotoxicity and pharmacological cardioprotection. *Antioxid. Redox Signal.* **18**, 899–929 (2013).
21. Patel, A. S. *et al.* Development and Validation of Endovascular Chemotherapy Filter Device for Removing High-Dose Doxorubicin: Preclinical Study. *Journal of Medical Devices* **8**, 041008 (2014).
22. Kim, H. Y. *et al.* A comparative study of high-dose hepatic arterial infusion chemotherapy and transarterial chemoembolization using doxorubicin for intractable, advanced hepatocellular carcinoma. *Korean J. Hepatol.* **16**, 355 (2010).
23. Gey G.O., Coffman W.D., Kubicek M.T. Tissue culture studies of the proliferative capacity of cervical carcinoma and normal epithelium. *Cancer Res.* **12**, 264–265 (1952).
24. Branco, A. F. *et al.* Differentiation-dependent doxorubicin toxicity on H9c2 cardiomyoblasts. *Cardiovasc. Toxicol.* **12**, 326–340 (2012).
25. Sardão, V. A., Oliveira, P. J., Holy, J., Oliveira, C. R. & Wallace, K. B. Morphological alterations induced by doxorubicin on H9c2 myoblasts: nuclear, mitochondrial, and cytoskeletal targets. *Cell Biol. Toxicol.* **25**, 227–243 (2009).
26. Qiu, M. *et al.* JS-K, a GST-activated nitric oxide donor prodrug, enhances chemosensitivity in renal carcinoma cells and prevents cardiac myocytes toxicity induced by Doxorubicin. *Cancer Chemother. Pharmacol.* **80**, 275–286 (2017).
27. Rharass, T. *et al.* Oxidative stress does not play a primary role in the toxicity induced with

- clinical doses of doxorubicin in myocardial H9c2 cells. *Mol. Cell. Biochem.* **413**, 199–215 (2016).
28. Arbo, M. D. *et al.* In vitro cardiotoxicity evaluation of graphene oxide. *Mutation Research/Genetic Toxicology and Environmental Mutagenesis* **841**, 8–13 (2019).
29. Singh, V. *et al.* Nitrogen doped carbon quantum dots demonstrate no toxicity under in vitro conditions in a cervical cell line and in vivo in Swiss albino mice. *Toxicol. Res.* **8**, 395–406 (2019).
30. Skalniak, L., Dziendziel, M. & Jura, J. MCPIP1 contributes to the toxicity of proteasome inhibitor MG-132 in HeLa cells by the inhibition of NF- $\kappa$ B. *Mol. Cell. Biochem.* **395**, 253 (2014).
31. Aziz, M. H. *et al.* Photodynamic Effect of Ni Nanotubes on an HeLa Cell Line. *PLoS One* **11**, (2016).
32. Lu, M. L., McCarron, R. J. & Jacobson, B. S. Initiation of HeLa cell adhesion to collagen is dependent upon collagen receptor upregulation, segregation to the basal plasma membrane, clustering and binding to the cytoskeleton. *J. Cell Sci.* **101 ( Pt 4)**, 873–883 (1992).
33. Hescheler, J. *et al.* Morphological, biochemical, and electrophysiological characterization of a clonal cell (H9c2) line from rat heart. *Circ. Res.* **69**, 1476–1486 (1991).
34. Aslantürk, Ö. S. In Vitro Cytotoxicity and Cell Viability Assays: Principles, Advantages, and Disadvantages. *Genotoxicity - A Predictable Risk to Our Actual World* (2018).  
doi:10.5772/intechopen.71923
35. Evans, H. M. & Schulemann, W. THE ACTION OF VITAL STAINS BELONGING TO THE BENZIDINE GROUP. *Science* **39**, 443–454 (1914).
36. Ra, H.-K. *et al.* A robust cell counting approach based on a normalized 2D cross-correlation

- scheme for in-line holographic images. *Lab Chip* **13**, 3398–3409 (2013).
37. O’Neil, E., Burton, S., Horney, B. & MacKenzie, A. Comparison of white and red blood cell estimates in urine sediment with hemocytometer and automated counts in dogs and cats. *Veterinary Clinical Pathology* **42**, 78–84 (2013).
  38. Li, L., Li, H.-S., Song, N.-N. & Chen, H.-M. The immunotoxicity of dibutyl phthalate on the macrophages in mice. *Immunopharmacology and Immunotoxicology* **35**, 272–281 (2013).
  39. Tsaousis, K. T. *et al.* Time-dependent morphological alterations and viability of cultured human trabecular cells after exposure to Trypan blue. *Clin. Experiment. Ophthalmol.* **41**, 484–490 (2013).
  40. Yip, D. K. & Auersperg, N. The dye-exclusion test for cell viability: persistence of differential staining following fixation. *In Vitro* **7**, 323–329 (1972).
  41. Mosmann, T. Rapid colorimetric assay for cellular growth and survival: Application to proliferation and cytotoxicity assays. *Journal of Immunological Methods* **65**, 55–63 (1983).
  42. Liu, Y., Peterson, D. A., Kimura, H. & Schubert, D. Mechanism of Cellular 3-(4,5-Dimethylthiazol-2-yl)-2,5-Diphenyltetrazolium Bromide (MTT) Reduction. *Journal of Neurochemistry* **69**, 581–593 (2002).
  43. Llovet, J. M. *et al.* Arterial embolisation or chemoembolisation versus symptomatic treatment in patients with unresectable hepatocellular carcinoma: a randomised controlled trial. *The Lancet* **359**, 1734–1739 (2002).
  44. Ferreira, L. L. *et al.* Single nanomolar doxorubicin exposure triggers compensatory mitochondrial responses in H9c2 cardiomyoblasts. *Food and Chemical Toxicology* **124**, 450–461 (2019).

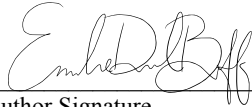
45. Pereira-Oliveira, M. *et al.* Doxorubicin Is Key for the Cardiotoxicity of FAC (5-Fluorouracil Adriamycin Cyclophosphamide) Combination in Differentiated H9c2 Cells. *Biomolecules* **9**, 21 (2019).

**Publishing Agreement**

*It is the policy of the University to encourage the distribution of all theses, dissertations, and manuscripts. Copies of all UCSF theses, dissertations, and manuscripts will be routed to the library via the Graduate Division. The library will make all theses, dissertations, and manuscripts accessible to the public and will preserve these to the best of their abilities, in perpetuity.*

***Please sign the following statement:***

*I hereby grant permission to the Graduate Division of the University of California, San Francisco to release copies of my thesis, dissertation, or manuscript to the Campus Library to provide access and preservation, in whole or in part, in perpetuity.*



\_\_\_\_\_  
Author Signature



\_\_\_\_\_  
Date